Electrochemical deposition of Pt nanoparticles on carbon nanotube patterns for glucose detection

Zeng, Zhiyuan; Zhou, Xiaozhu; Huang, Xiao; Wang, Zhijuan; Zhang, Qichun; Yang, Yanli; Boey, Freddy Yin Chiang; Zhang, Hua

2010

Zeng, Z., Zhou, X., Huang, X., Wang, Z., Yang, Y., Zhang, Q., et al. (2010). Electrochemical deposition of Pt nanoparticles on carbon nanotube patterns for glucose detection. Analyst, 135, 1726–1730.

https://hdl.handle.net/10356/93938

https://doi.org/10.1039/c000316f

Electrochemical deposition of Pt nanoparticles on carbon nanotube patterns for glucose detection†

Zhiyuan Zeng,[a] Xiaozhu Zhou,[a] Xiao Huang,[a] Zhijuan Wang,[a] Yanli Yang,[ab] Qichun Zhang,[a] Freddy Boey[ab] and Hua Zhang*[ab]

Received (in XXX, XXX) Xth XXXXXXXXX 20XX, Accepted Xth XXXXXXXXX 20XX
DOI: 10.1039/b000000x

Single-walled carbon nanotube (SWCNT) microarrays are successfully patterned on SiO_2 substrates based on an evaporation-induced self-assembly mechanism. On these SWCNT micropatterns, the highly electroactive polycrystalline Pt nanoparticles (PtNPs) are deposited by using the electrochemical method. The obtained PtNP-SWCNT nanocomposites exhibit a low detection limit for hydrogen peroxide (4 μM). The further investigation on a glucose oxidase (GOx)/BSA/PtNP-SWCNT based biosensor indicates that the detection limit and sensitivity for glucose are 0.04 mM and 4.54 μA mM^{-1} cm^{-2}, respectively. Our results prove that the improved electrocatalytic activity originates from the PtNP-SWCNT micropatterns, which provide a potential platform to immobilize different enzymes used for bioelectrochemical applications.

Introduction

Single-walled carbon nanotubes (SWCNTs) and their patterns have attracted increased attention, because of their high electroactive effect, fast electron transfer rate, high chemical stability, and high surface-to-volume ratios,[1–5] as well as many potential applications in flat panel displays, nanoelectronics, sensors, and metal catalyst supports.[6] Till now, several techniques such as photolithography,[7] e-beam lithography,[8] soft-lithography,[9,10] dip-pen nanolithography,[10a] and scratching methods[10b,c] have been reported to pattern CNTs on various substrates. Unfortunately, these patterning processes are relatively complicated[7–9,10a] and/or the resultant density of CNT arrays is usually relatively low.[7–10] Therefore, the development of a simple method for patterning highly dense and spontaneously aligned CNTs on solid substrates is required.

Although the deposition of metal NPs onto CNTs is difficult due to the CNT's inherent properties such as hydrophobic property,[11] small size, high curvature and chemical inertness, the electrochemical deposition has been proven to be an efficient method to prepare metal nanostructured materials. The electrochemical behaviors and applications of the deposited noble metal NPs have been investigated in carbon-based electrodes, including Au/Pd-SWCNT,[12] Pt-MWCNT,[13,14] and Pt-CNT/graphite electrodes.[15] Recently, using nafion as a binding agent, Pt nanoparticles (PtNP)-SWCNT composites have been successfully used for electrochemical biosensors.[16] However, the use of nafion makes the preparation process tedious and complicated.

Herein, we report the electrochemical deposition of PtNPs onto SWCNT microarrays, which are then used as biosensors for detection of glucose. The SWCNT microarrays were prepared based on a simple evaporation-induced self-assembly method. The advantages of the SWCNT microarrays are that they can not only provide the possibility for massively parallel analysis,[17,18] but also exhibit higher sensitivity, lower detection limit, and improved signal-to-noise (S/N) ratio.[19,20] After the integration of PtNPs and SWCNT microarrays through the direct electrochemical deposition, the amperometric biosensor was successfully fabricated by deposition of 211 units of glucose oxidase (GO_X) on this electrode. Our results prove that the PtNP-SWCNT electrode is a potential platform for immobilization of different enzymes, which can be used for the bioelectrochemical applications.

Methods

Materials

SWCNTs (P3) were purchased from Carbon Solutions, Inc. (CA, USA). Glucose oxidase (GOx, EC 1.1.3.4, from Aspergillus niger, 211 units/mg), glutaraldehyde (50%), potassium hexacyanoferrate (II) ($K_4Fe(CN)_6$, 99.5%), hydrogen peroxide (35%), bovine serum albumin (BSA), D(+)-glucose (99.5%), potassium hexachloroplatinate (K_2PtCl_6), perchloric acid (70%), and phosphate buffer saline tablets were purchased from Aldrich (Milwaukee, WI, USA) and used as received. The supporting electrolyte is 10 mM phosphate buffer (pH = 7.4). All chemicals are of analytical grade and all the solutions are prepared using Milli-Q water (18.2 MΩ cm, Milli-Q System, Millipore, Billerica, MA, USA).

Instruments

Cyclic voltammetric and amperometric experiments were performed on a CHI 660C electrochemical workstation (CH

[a]*School of Materials Science and Engineering, Nanyang Technological University, 50 Nanyang Avenue, Singapore 639798. E-mail: HZhang@ntu.edu.sg; HZhang166@yahoo.com.; Web: http://www.ntu.edu.sg/home/hzhang/; Fax: (+65) 6790 9081; Tel: (+65) 6790 5175*
[b]*Centre for Biomimetic Sensor Science, Nanyang Technological University, 50 Nanyang Drive, Singapore 637553*
† Electronic supplementary information (ESI) available: Further experimental results. See DOI: 10.1039/c000316f/

Instrument, Austin, TX, USA) with a conventional three-electrode cell, where the PtNP-modified SWCNT patterns on SiO_2, a Pt wire, and a Ag/AgCl (sat. KCl) electrode were used as working, counter, and reference electrode, referred to as WE, CE and RE, respectively. The amperometric experiments were performed in the stirring electrolyte solutions at 25 °C. The TEM images were obtained from a transmission electron microscope (JEOL JEM-2100, Tokyo, Japan). SEM was performed using a JEOL JSM-6700 field-emission scanning electron microanalyzer (Tokyo, Japan) at an accelerating voltage of 1.0 and 10.0 keV, respectively.

Fabrication of SWCNT patterns

The fabrication process of SWCNT patterns is shown in Scheme 1. After the cleaned SiO_2 substrate was immersed in a beaker containing the purified CNT solution (concentration: 0.004 mg mL^{-1}) at a tilting angle of *ca.* 15°, the beaker was placed in an oven at 80 °C until the solution evaporated to dryness. The SWCNT patterns on SiO_2 were obtained, which were then annealed in a furnace at 350 °C for 3 h under the nitrogen atmosphere. Finally, a contact Au electrode (2 × 4.8 mm^2, 60 nm of Au with a 10 nm Cr as an adhesive layer) was coated to cover one end of the SWCNT line patterns (7 × 4.8 mm^2), see the electrode in Scheme 1.

Preparation of PtNP-SWCNT nanocomposites

The electrochemical deposition of PtNPs was performed in a three-electrode cell using the patterned SWCNTs, Ag/AgCl (sat. KCl), and Pt wire as WE, RE, and CE, respectively. Prior to use, the patterned SWCNT electrode was thoroughly washed with ethanol and then water. The deposition of PtNPs on SWCNT patterns, from a solution containing 2 mM K_2PtCl_6 and 0.5 M perchloric acid, followed the method described in a previous report,[21] with a deposition potential of −0.4 V (vs. Ag/AgCl) and time of 30 s.

Fabrication of GOx/BSA/PtNP-SWCNT based sensors

The fabrication process of the GOx/BSA/PtNP-SWCNT based biosensor is shown in Scheme 2. The enzyme solution was prepared by mixing 10 mg of glucose oxidase (GOx) and 5 mg of bovine serum albumin (BSA) in a 1 mL 10 mM phosphate buffer. 3 μL of thus-prepared enzyme solution was dropped on the PtNP-SWCNT electrode. After it dried, glutaraldehyde (3.0 μL, 2.5%) was coated on the resulting electrode used for cross-linking the enzymes. The as-prepared electrode was stored in 10 mM phosphate buffer (pH 7.4) at 4 °C. Amperometry was performed in a 10 mM phosphate buffer (pH 7.4). The stock solutions of different concentration of anhydrous D-glucose were prepared in 10 mM phosphate buffer (pH 7.4) and stored at 4 °C (mutarotation was allowed for at least 24 h before use).[16] The active surface area of the electrode before and after enzyme immobilization was determined by cyclic voltammetry for a mixed solution containing 20 mM $K_4Fe(CN)_6$ and 0.2 M potassium chloride.

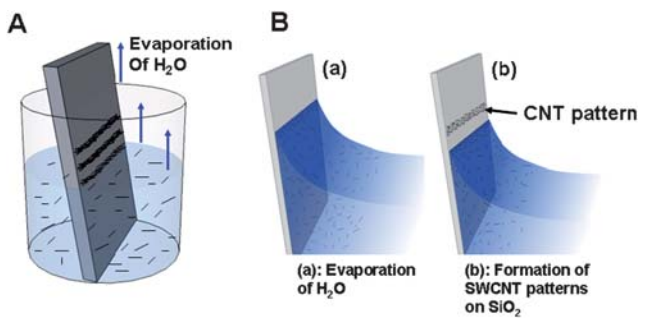

Scheme 1 Schematic illustration of SWCNT patterns on SiO_2 formed by the evaporation-induced self-assembly mechanism.

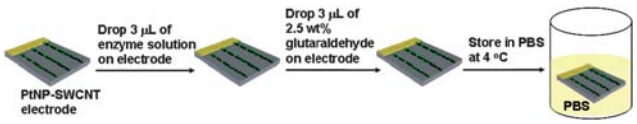

Scheme 2 Preparation of GOx/BSA/PtNP-SWCNT based glucose biosensor.

Results and discussion

Formation mechanism of SWCNT patterns

Scheme 1 shows how the SWCNT patterns form on a SiO_2 substrate. The formation mechanism can be proposed as follows. With the evaporation of H_2O, *i.e.* the solvent of SWCNTs, the contact angle of H_2O on the SiO_2 substrate decreases, resulting in the increase of capillary force.[22] When the capillary force increases to a certain value, and cannot hold the adsorbed H_2O layer on SiO_2 surface due to the continuous evaporation of H_2O, the adsorbed H_2O layer on SiO_2 will drastically drop a certain distance and leave some SWCNT solution on SiO_2. The SWCNTs then self-assemble to form a SWCNT line (Scheme 1B). Large-area SWCNT line patterns can be obtained after the aforementioned process repeats until H_2O is dried. As such, the substrate plays a critical role in the formation of SWCNT patterns. Based on our experiment, it was found that only hydrophilic surface allows the formation of SWCNT patterns. Note that the relatively high incubation temperature (80 °C used in our experiment) favors the formation of SWCNT patterns.

Characterization of PtNP-SWCNT composites

Fig. 1A shows a large-area SEM image of the self-assembled SWCNT patterns on SiO_2. The inset in Fig. 1A clearly shows that the as-prepared arrays comprised of densely packed SWCNTs. The average width of the SWCNT line patterns is *ca.* 8 μm. Fig. 1B shows the SEM image of highly dense PtNP-decorated SWCNT arrays, prepared by the electrochemical deposition method. A magnified field-emission SEM image, typically recorded at 10 kV, was used to clearly identify the PtNPs (Fig. 1C), which were also confirmed by energy dispersive X-ray analysis (EDS, bottom left inset in Fig. 1C). The measured size of PtNPs is 75.5 ± 10.3 nm (top right inset in Fig. 1C), which is consistent with the result obtained by TEM (average diameter ~75.5 nm, Fig. 2A). The selected area electron diffraction pattern (SAED, inset in Fig. 2A) on one PtNP exhibits the discontinuous diffraction rings. The 3 innermost rings can be

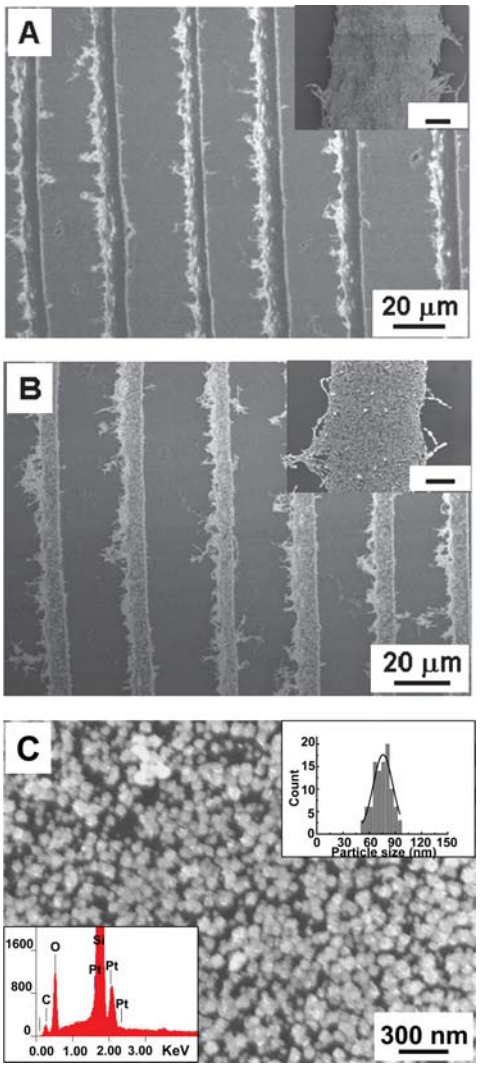

Fig. 1 SEM images of SWCNT patterns on SiO_2 before electrochemical deposition of PtNPs (A, inset: magnified image, scale bar = 2 μm), and after electrochemical deposition of PtNPs (B, inset: magnified image, scale bar = 2 μm). (C) High magnification of PtNPs deposited on SWCNT patterns, insets: EDS of PtNPs deposited on SWCNT patterns (bottom left), and size distribution of PtNPs deposited on SWCNT patterns (top right).

assigned to {111}, {002}, and {011} reflections of *fcc* Pt. Therefore, the electrochemical deposited PtNPs are polycrystalline, which are further confirmed by a high resolution TEM image of the edge portion of one PtNP (Fig. 2B). In one of the polycrystalline domains, the measured lattice spacings are 2.0 and 2.3 Å, corresponding to the (002) and (111) planes, respectively, suggesting that this domain is oriented along the <110> direction.

Estimation of the electroactive surface area of PtNP-SWCNT electrodes

Fig. 3 shows the cyclic voltammograms (CVs) of the PtNP-SWCNT electrode (a) and the patterned SWCNT electrode (b) in a 0.2 M KCl solution containing 20 mM $[Fe(CN)_6]^{3-/4-}$, at a scan

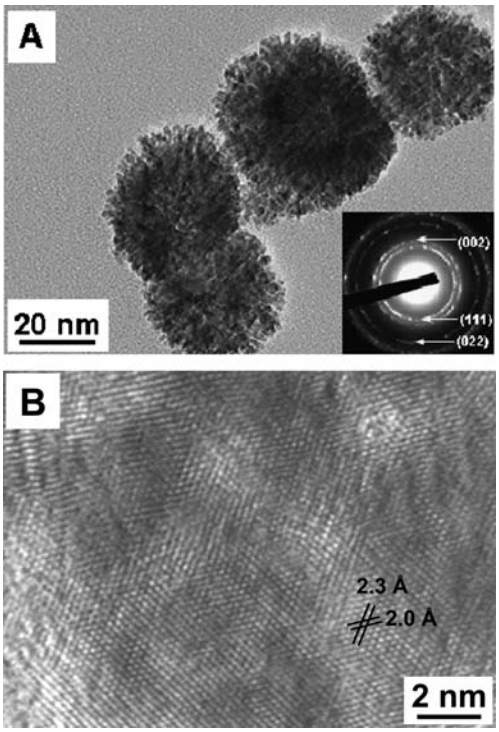

Fig. 2 (A) TEM image of polycrystalline PtNPs. Inset: SAED pattern on a typical PtNP. (B) HRTEM image of the edge portion of a typical PtNP.

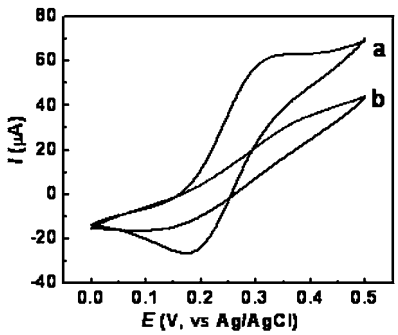

Fig. 3 Estimation of electroactive surface area of (a) PtNP-SWCNT and (b) patterned SWCNT electrodes by cyclic voltammetry in a mixed solution containing 20 mM $[Fe(CN)_6]^{3-/4-}$ and 0.2 M KCl at a scan rate of 10 mV s^{-1}.

rate of 10 mV s^{-1}. The well-defined oxidation and reduction peaks of the PtNP-SWCNT electrode at + 0.33 and + 0.18 V are attributed to the forward and reverse scans of Fe^{3+}/Fe^{2+} redox couple, respectively. The surface area of the PtNP-SWCNT electrode can be calculated according to the Randles–Sevcik equation,[16]

$$I_p = 2.69 \times 10^5 AD^{1/2}n^{3/2}\gamma^{1/2}C \quad (1)$$

where n is the number of electrons participating in the reaction and is equal to 1 here, A denotes the area of the electrode (cm^2), D is the diffusion coefficient of the molecule in solution (6.70×10^{-6} cm^2 s^{-1}),[16] C is the concentration of the probe molecule in

the solution, and γ is the scan rate (V s^{-1}). The electroactive surface area has a linear function with the peak current of the redox couple. The calculated average values of the electroactive surface area were 3.82×10^{-2} and 1.77×10^{-2} cm^2 for the PtNP-SWCNT and patterned SWCNT electrode, respectively. Clearly, the PtNP-SWCNT electrode has a much higher electroactive surface area than the patterned SWCNT electrode, due to the decoration of highly catalytic PtNPs.

Detection of hydrogen peroxide using PtNP-SWCNT electrode

Fig. 4 presents a typical current-time curve of PtNP-SWCNT electrode with successive additions of H_2O_2 at + 0.55 V. A quick response can be observed at the electrode with a steady-state current to be reached within 3 s after addition of H_2O_2. The PtNP-SWCNT electrode can detect the H_2O_2 concentration as low as 4 μM with a sensitivity of 0.11 A M^{-1} cm^{-2}. The H_2O_2 detection with PtNP-SWCNT electrode typically exhibits a linear range from 4 μM to 0.84 mM ($R^2 = 0.9920$). The detection limit is lower than that using mesoporous Pt electrode (4.5 μM)[23] and SWCNT pattern electrode (15 μM, as shown in Figure S1†). This low detection limit, benefiting from the porous and polycrystalline PtNPs through the direct electrochemical deposition, is due to an increase in the ratio of surface atoms with free valances to the total atoms of PtNPs.[12,16,24] Moreover, the patterned SWCNT arrays can also improve the detection limit.[19,20]

Detection of glucose using GOx/BSA/PtNP-SWCNT electrode

Fig. 5 shows a typical current-time curve of the GOx modified PtNP-SWCNT electrode upon the successive addition of glucose at + 0.55 V. In the plot, the response current increases with the concentration of glucose, and finally reaches a steady state. The response time of the enzyme towards glucose is less than 20 s when a steady state current is reached. The GOx/BSA/PtNP-SWCNT electrode exhibits linearity with the glucose concentration from 0.04 to 0.87 mM. The linear range is wider than that in Pt-MWCNT[14] and Pt-CNT/graphite electrodes.[15] The sensitivity and detection limit of GOx/BSA/PtNP-SWCNT electrodes

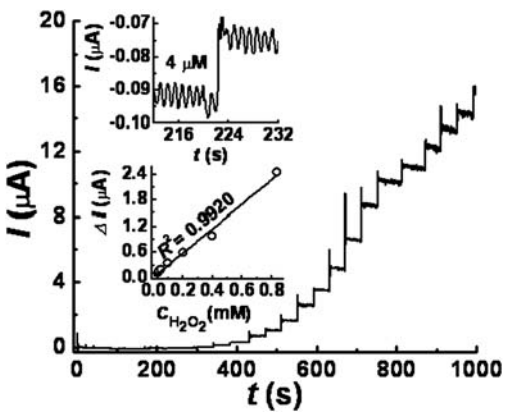

Fig. 4 Performance of PtNP-SWCNT electrode in amperometric detection of H_2O_2 at +0.55 V *vs.* Ag/AgCl (sat. KCl). Inset: a detection limit of 4 μM with S/N = 3 (top), and the calibration curve at H_2O_2 concentration between 4 μM and 0.84 mM (bottom).

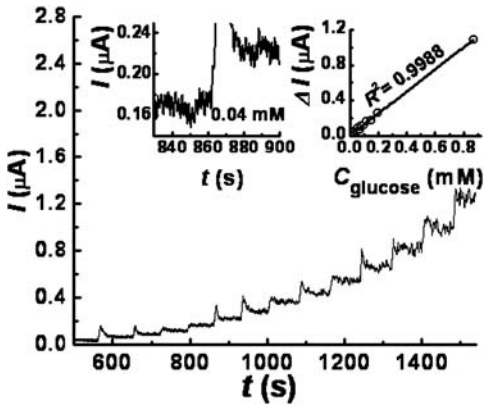

Fig. 5 Amperometric response of GOx/BSA/PtNP-SWCNT electrode upon successive additions of glucose solution in a 10 mM phosphate buffer (pH 7.4) at + 0.55 V *vs.* Ag/AgCl (sat. KCl) at 25 °C. Inset: detection limit of 0.04 mM (left), and the calibration curve at glucose concentration between 0.04 and 0.87 mM (right).

are 4.54 A mM^{-1} cm^{-2} ($R^2 = 0.9988$) and 0.04 mM, respectively. The detection limit shown here is lower than the GOx/BSA/SWCNT electrode (0.08 mM, as shown in Figure S2†). On the other hand, the GOx/BSA/SWCNT electrode shows almost no response to the addition of the high concentration glucose, if there is no redox mediator (such as *p*-benzoquinone). As a result, the hybridization of PtNPs with SWCNT patterns not only increases the electroactive surface of the electrode, but also enhances the catalytic property of the electrode. Therefore, the operating potential decreases and the current signal when adding glucose is obtained without the addition of a redox mediator. The detection limit of the GOx/BSA/PtNP-SWCNT electrode used here is lower than that of other comparable CNT materials (0.05 mM),[25] CNT nanoelectrode ensembles (0.08 mM),[20] Nafion/GOx/PtNP/CNT/Graphite (0.1 mM),[26] and Pt-MWCNT (0.4 mM).[13] Also, the sensitivity of our PtNP-SWCNT electrode is much better than that of CNT (0.27 A mM^{-1} cm^{-2}) and Pt-CNT paste (0.98 A mM^{-1} cm^{-2}) based biosensors.[27] Such a lower detection limit and high sensitivity originate from the integration of PtNPs and SWCNT patterns. Our results prove that PtNPs are promising candidates for glucose sensing, since they can act as electrocatalysts in the oxidation/reduction of H_2O_2,[16] and facilitate the direct electron transfer between the enzyme and the electrode surface.

The apparent Michaelis–Menten constant (k_m^{app}), an indication of the enzyme-substrate kinetics[28] in the glucose biosensor, can be calculated from the Lineweaver-Bulk equation,[29] as shown in eqn (2):

$$\frac{1}{i_s} = \left(\frac{K_m^{app}}{i_{max}}\right)\left(\frac{1}{C}\right) + \left(\frac{1}{i_{max}}\right) \quad (2)$$

where i_s is the steady-state current, C is the concentration of glucose, k_m^{app} is the apparent Michaelis–Menten constant, and i_{max} is the maximum current. From eqn (2), the k_m and i_{max} are estimated to be 0.68 mM and 27.87 μA cm^{-2}, respectively. Since the smaller k_m means the higher enzymatic activity of the immobilized GOx, and a higher glucose-affinity in the electrode,[30] our PtNP-SWCNT electrode shows a better result than the Pt-MWCNT electrode (11.02 mM).[14]

Conclusions

In summary, a simple and effective method based on the evaporation-induced self-assembly mechanism is used to pattern the dense SWCNT arrays on SiO_2 substrates. The as-prepared SWCNT patterns can be used as electrodes for electrochemical deposition of the electroactive and polycrystalline Pt nanoparticles (PtNPs). The resulting PtNP-SWCNT electrode exhibits a lower detection limit (4 μM) towards hydrogen peroxide, which renders it a good platform for the oxidase-based biosensing. Furthermore, a new biosensor based on the GOx/BSA/PtNP-SWCNT electrode shows good glucose detection capability, with the detection limit of 0.04 mM and a sensitivity of 4.54 $\mu A\ mM^{-1}\ cm^{-2}$. Our results clearly show that this type of sensor holds many advantages at low applied potentials, such as the high sensitivity, low detection limit, high reproducibility, and fast current response.

Acknowledgements

This work was supported by a Start-Up Grant from NTU, AcRF Tier 1 (RG 20/07) from MOE, POC (S08/1-82563404) from EDB, CRP (NRF-CRP2-2007-01) from NRF, an A*STAR SERC Grant (No. 092 101 0064) from A*STAR, and the Centre for Biomimetic Sensor Science at NTU in Singapore.

Notes and references

1 M. Musameh, J. Wang, A. Merkoci and Y. H. Lin, *Electrochem. Commun.*, 2002, **4**, 743.
2 J. X. Wang, M. X. Li, Z. J. Shi, N. Q. Li and Z. N. Gu, *Anal. Chem.*, 2002, **74**, 1993.
3 J. Wang, M. Musameh and Y. H. Lin, *J. Am. Chem. Soc.*, 2003, **125**, 2408.
4 J. Wang and M. Musameh, *Anal. Chem.*, 2003, **75**, 2075.
5 H. Dai, *Acc. Chem. Res.*, 2002, **35**, 1035.
6 P. Avouris, *Acc. Chem. Res.*, 2002, **35**, 1026.
7 N. R. Franklin, Y. M. Li, R. J. Chen, A. Javey and H. Dai, *Appl. Phys. Lett.*, 2001, **79**, 4571.
8 M. Haffner, A. Haug, R. T. Weitz, M. Fleischer, M. Burghard, H. Peisert, T. Chasse and D. P. Kern, *Microelectron. Eng.*, 2008, **85**, 768.
9 (*a*) H. Kind, J. M. Bonard, C. Emmenegger, L. O. Nilsson, K. Hernadi, E. Maillard-Schaller, L. Schlapbach, L. Forro and K. Kern, *Adv. Mater.*, 1999, **11**, 1285; (*b*) S. M. Huang, A. W. H. Mau, T. W. Turney, P. A. White and L. M. Dai, *J. Phys. Chem. B.*, 2000, **104**, 2193.
10 (*a*) B. Li, C. F. Goh, X. Zhou, G. Lu, H. Tantang, Y. Chen, C. Xue, F. Y. C. Boey and H. Zhang, *Adv. Mater.*, 2008, **20**, 4873; (*b*) B. Li, X. Cao, X. Huang, G. Lu, Y. Huang, C. F. Goh, F. Y. C. Boey and H. Zhang, *Small*, 2009, **5**, 2061; (*c*) X. Cao, B. Li, Y. Huang, F. Boey, T. Yu, Z. X. Shen and H. Zhang, *ACS Appl. Mater. Interfaces*, 2009, **1**, 1873.
11 E. Dujardin, T. Ebbesen, W. H. Hiura and K. Tanigaki, *Science*, 1994, **265**, 1850.
12 J. C. Claussen, A. D. Franklin, A. ul Haque, D. M. Porterfield and T. S. Fisher, *ACS Nano*, 2009, **3**, 37.
13 X. Chu, D. X. Duan, G. L. Shen and R. Q. Yu, *Talanta*, 2007, **71**, 2040.
14 M.-C. Tsai and Y.-C. Tsai, *Sens. Actuators, B*, 2009, **141**, 592.
15 H. Tang, J. H. Chen, S. Z. Yao, L. H. Nie, G. H. Deng and Y. F. Kuang, *Anal. Biochem.*, 2004, **331**, 89.
16 S. Hrapovic, Y. L. Liu, K. B. Male and J. H. T. Luong, *Anal. Chem.*, 2004, **76**, 1083.
17 J. B. Delehanty and F. S. Ligler, *Anal. Chem.*, 2002, **74**, 5681.
18 C. A. Rowe-Taitt, J. P. Golden, M. J. Feldstein, J. J. Cras, K. E. Hoffman and F. S. Ligler, *Biosens. Bioelectron.*, 2000, **14**, 785.
19 Y. Tu, Y. H. Lin and Z. F. Ren, *Nano Lett.*, 2003, **3**, 107.
20 Y. H. Lin, F. Lu, Y. Tu and Z. F. Ren, *Nano Lett.*, 2004, **4**, 191.
21 T. M. Day, P. R. Unwin, N. R. Wilson and J. V. Macpherson, *J. Am. Chem. Soc.*, 2005, **127**, 10639.
22 T. Niiyama and Kawai, *Microelectron. Eng.*, 2006, **83**, 1280.
23 S. A. G. Evans, J. M. Elliott, L. M. Andrews, P. N. Bartlett, P. J. Doyle and G. Denuault, *Anal. Chem.*, 2002, **74**, 1322.
24 K. Balasubramanian and M. Burghard, *Anal. Bioanal. Chem.*, 2006, **385**, 452.
25 Y. L. Yao and K. K. Shiu, *Anal. Bioanal. Chem.*, 2007, **387**, 303.
26 H. Tang, J. H. Chen, S. Z. Yao, L. H. Nie, G. H. Deng and Y. F. Kuang, *Anal. Biochem.*, 2004, **331**, 89.
27 M. H. Yang, Y. H. Yang, Y. L. Liu, G. L. Shen and R. Q. Yu, *Biosens. Bioelectron.*, 2006, **21**, 1125.
28 B. Y. Wu, S. H. Hou, F. Yin, J. Li, Z. X. Zhao, J. D. Huang and Q. Chen, *Biosens. Bioelectron.*, 2007, **22**, 838.
29 R. A. Kamin and G. S. Wilson, *Anal. Chem.*, 1980, **52**, 1198.
30 X. Kang, J. Wang, H. Wu, ilhan A. Aksay, J. Liu and Y. Lin, *Biosens. Bioelectron.*, 2009, **25**, 901.